www.czasopisma.pan.pl PAN POLSKA AKADEMIA NAUK www.journals.pan.pl

A R C H I V E S O F M E T A L L U R G Y A N D M A T E R I A L S

Volume 56 2011 Issue 3

DOI: 10.2478/v10172-011-0088-7

R. WŁODARCZYK*, A. DUDEK*

SINTERED MATERIALS FOR BIPOLAR PLATES

MATERIAŁY SPIEKANE PRZEZNACZONE NA PŁYTY BIPOLARNE

This study presents an analysis of opportunities of the application of stainless steel for interconnectors in fuel cells. The investigations also included microstructural analysis of sintered materials in terms of use of them as interconnectors in proton exchange membrane fuel cells (PEMFC). Corrosion resistance in sinters made of a stainless steel was analysed in sulphate solutions; general corrosion resistance and pitting corrosion resistance were tested in the presence of chloride ions. Due to the multifunctionality of materials for interconnectors, selection of these materials is extremely difficult. Results of the investigations of corrosion resistance prove that corrosion resistance is connected with the structure of material and chemical composition of sinters.

Keywords: fuel cell, bipolar plates, corrosion, sintered steel

Niniejsze wyniki badań przedstawiają możliwość zastosowania stali nierdzewnej na okładki ogniw paliwowych. W pracy przedstawiono również wyniki badań mikrostrukturalnych materiałów spiekanych do wykorzystania jako interkonektory w ogniwach paliwowych z elektrolitem w postaci membrany protonowymiennej. Opór polaryzacji materiałów spiekanych był określony w wyniku badań korozyjnych w roztworach siarczanowych - korozja ogólna, szybkość korozji wżerowej badano w obecności jonów chlorkowych. Ze względu na wielofunkcyjność materiałów na okładki, dobór materiałów na te elementy jest niezwykle trudny. Wyniki badań korozyjnych wskazują zależność od struktury materiału oraz składu chemicznego spieków.

1. Introduction

The world demand for energy is still on the increase. As compared to 2006, the Earth's population in 2023 is estimated to rise by 24% while number of vehicles moving around the planet will increase by 50%. This tendency means that the world production of crude oil and natural gas would have to rise by 66% to cover the expected demand. These will happen to the detriment of the environment and climate. The most optimistic scenarios among geologists and petrochemical industry specialists assume that oil industry recession will occur in our generation's lifetime. This implies that the peak crude oil production will take place whereas oil demand will exceed its production, which will result in corresponding increase in prices for this fuel. Contrary to the popular belief, each aspect of our lifestyle is associated with consumption of petrochemicals and fossil fuels; food manufacturing, water procurement, medicine, civil engineering, all of them rely on oil supplies. Facing end of era of oil, our destiny is to search for new areas of energy acquisition.

Among many solutions to generate energy, use of fuel cells to generate electricity and heat should be emphasised [1-2]. Fig. 1 presents the model of fuel cell with cylindrical electrodes. As can be observed from Fig. 1, single fuel cell is composed of the anode, cathode and electrolyte/membrane located between them.

* DEPARTMENT OF ENERGY ENGINEERING, CZESTOCHOWA UNIVERSITY OF TECHNOLOGY, 42-200 CZĘSTOCHOWA, 60A BEREŹNICKA STR., POLAND
* INSTITUTE OF MATERIALS ENGINEERING, CZESTOCHOWA UNIVERSITY OF TECHNOLOGY, 42-200 CZĘSTOCHOWA, POLAND

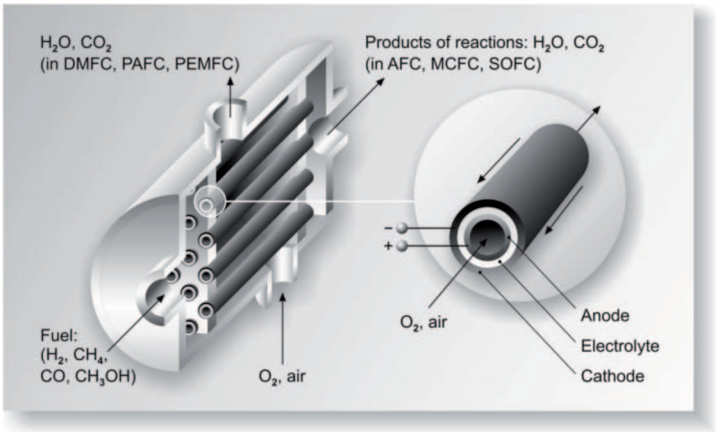

Fig. 1. Structure of fuel cell with cylindrical electrodes in the form of pipes

Such elements are then arranged into stacks and placed in the interconnectors (not shown in Fig. 1). Interconnectors for fuel cells are a specific part of PEMFC stack since it comprises *ca.* 80% of total weight and 45% of stack cost. Bipolar plates are designed to accomplish many functions, such as uniform distribution of reactant over the active areas, removal of heat from active areas, carrying current from cell to cell and prevention of leakage of reactants and coolant. Furthermore, the plates must be inexpensive, made of light materials and must be easily manufactured.

Variety of fuel cells proves opportunities of development of these cells with consideration of new materials for anode, cathode and electrolyte as well as solutions concerning interconnectors for PEMFC. Nowadays, many research centres focus on investigations of extending of their lifetime, decreasing the weight of the equipment or reduction in manufacturing costs [3-9].

Fuel cells are said to be environmentally friendly since the released gases, except water (hydrogen cells) and carbon dioxide (methanol-based cells), do not contain harmful substances, which is a result of stringent requirements imposed on fuel purity. Fuel cells are noiseless, do not contain moving parts which are common source of noise. The only noise comes from fuel cell auxiliary equipment. Fuel cells can be used as home electricity generators, uninterruptible power supply (UPS) systems or emergency electricity generators for hospitals [10-13].

This paper presents opportunities of application of a new technology of powder sintering for creation of parts for electricity and heat generators. Sintering stainless steel of 304L, 316L, and 434L were studied as candidate bipolar plate materials. Opportunities for use stainless steel sinters were analyzed based on morhological and microstructure examinations. In order to determine the resistance to corrosion in the environment of fuel cell's work, potentiokinetic curves were registered in several solutions: 0.5 mol dm^{-3} solution of H_2SO_4; 0.5 mol dm^{-3} solution of Na_2SO_4 and 0.5 mol dm^{-3} Na_2SO_4+0.5 mol dm^{-3} NaCl.

2. Experimental part

The investigations encompassed sinters with composition given in Table. 1. The powders were compacted with the following load: 705 MPa for 304LHD powder, 700 MPa for 316LHD powder and 765 MPa for 434LHC powder and sintered at the temperature of 1250 °C for 30 minutes in ammonia medium.

TABLE 1
Chemical composition of the powders used for sintering

Powder Grade	C [%]	Mo [%]	Ni [%]	Cr [%]	Si [%]	Mn [%]	Fe [%]
304LHD	0.013	–	11.2	18.9	0.9	0.1	balance
316LHD	0.025	2.2	12.3	16.7	0.9	0.1	balance
434 LHC	0.015	0.98	–	16.2	0.8	0.1	balance

In order to determine anticorrosion properties in sintered materials, polarization curves were registered in the following solutions: 0.5 mol dm^{-3} solution of H_2SO_4, 0.5 mol dm^{-3} solution of Na_2SO_4 and 0.5 mol dm^{-3} Na_2SO_4+0.5 mol dm^{-3} NaCl with measurement rate of 1 mV s^{-1}. On the basis of polarization curves, the parameters which define corrosion resistance of the material were determined, i.e. corrosion potential E_{corr}, polarization resistance R_p, corrosion current density i_{corr}. The most representative polarization curves were used for analysis of corrosion resistance. Electrochemical measurements were carried out in three-electrode arrangement by means of CHI660 (CH Instruments USA) measurement unit. Reference electrode was formed by satu-

rated calomel electrode (SCE) while auxiliary electrode was platinum wire. The sample was then placed just above the tip of the luggin capillary (approximately 2-3 mm). All chemicals were reagent grade and were used as received without further purification. Distilled and subsequently deionized water was used to prepare test solutions. Scanning electron microscopy (SEM) images were obtained using JOEL Model JSM-5400. An analysis of the surface of sintered materials after exposition in corrosion solution was carried out by means of Axiovert optical microscope.

3. Test results and discussion

3.1. Microstructural tests

Analysis of morphology in the used powders revealed that they were characterized by comparable diameter of *ca.* 50 μm and density of *ca.* 2.6 g/cm^3. The microstructure of the powders used for preparation of the sinters is presented in Fig. 2.

Distribution of powder particles size is presented by means of histogram presented in Fig. 3. A fundamental geometrical parameter which determines powders is the size of its particles. The used powders, as results from the microscope analysis, are characterized by irregular, dendritic structure. Particular functional parameters of the investigated powders allowed for determination of physicochemical properties of the powders. These properties depend directly on the method of powder preparation. The 304LHD and 316LHD powders show comparable values of grains (Fig. 2, Fig. 3), in contrast to the 434LHC powder. Evaluation of the shape, size and distribution of the particles was carried out by means of computer-aided image analysis. The results are presented in the form of histogram (see Fig. 3).

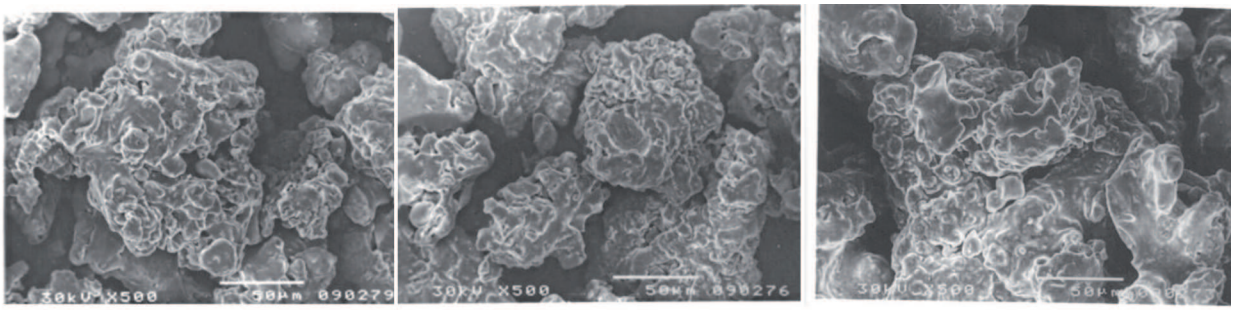

A B C

Fig. 2. Microstructure of 304LHD, 316LHD, 434LHC powder. Magnification 500x

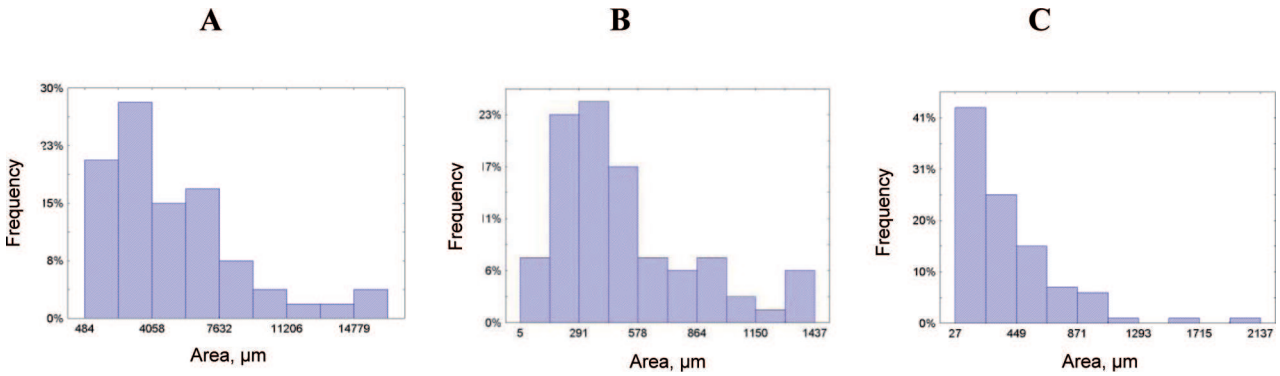

Fig. 3. Histogram of surface area in 304LHD, 316LHD, 434LHC powders particles

4. Corrosion resistance tests

In order to analyse corrosion resistance of the sintered materials, polarization curves were registered in 0.5 mol dm^{-3} solution of H_2SO_4 (Fig. 4A). As results from polarization curves profiles, the investigated materials are subjected to passivation in the corrosion solution. The highest value of current density in the initial point of passivation is observed for the sinter with the ferritic structure, 434L (i_{pass}=4.58 mA cm^{-2}). This sinter is also characterized by the lowest value of current density in passive range, *ca*. 0.05 mA cm^{-2}, 0.07 mA cm^{-2} for 304L and 0.13 mA cm^{-2} for 316L. Fig. 4B presents the value of polarization resistance for sintered materials. According to the Stern-Hoar equation, external current density within the range of potentials that insignificantly differ from corrosion potential (± 20 mV) is a linear function of potential [14]. Slope of the line ΔE=f(Δi) is a measure of polarization resistance. The analysis of the value of polarization resistance determined on the basis of the data presented in Fig. 4A reveals that the highest corrosion resistance is observed for the 316L sinter.

Profiles of potentiokinetic curves recorded for the sintered materials in 0.5 mol dm^{-3} sinter of Na_2SO_4 are presented in Fig. 5A. Fig. 5B presents the values of polarization resistance for the analysed sinters on the basis of potentiokinetic curves.

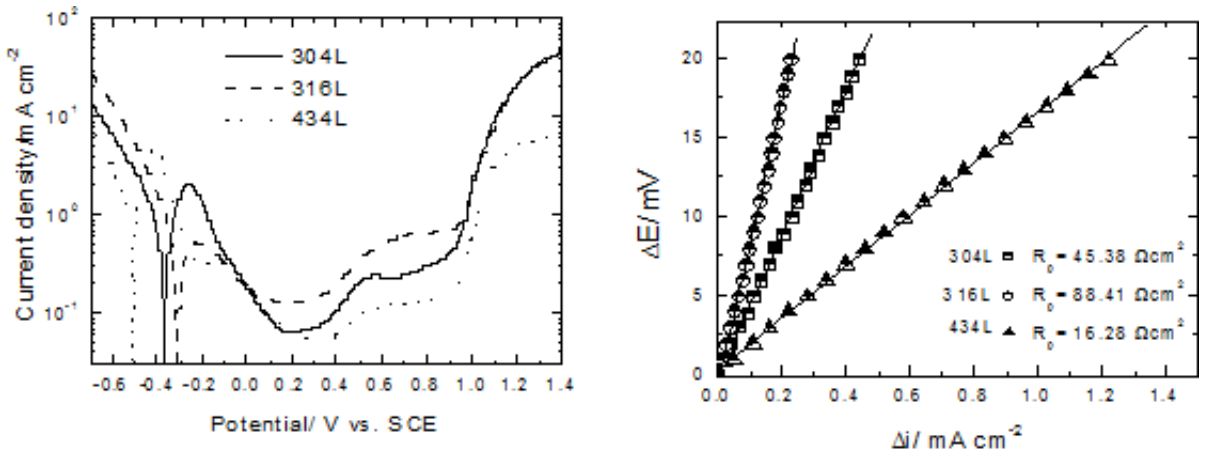

Fig. 4. A) Anodic polarization curves for the sintered stainless steel obtained in 0.5 mol dm^{-3} H_2SO_4, scan rate 1 mV s^{-1}, B) Change in the value of external current as a function of the applied voltage (within the range of E_{corr} + ΔE) for the analysed sinters on the basis of potentiokinetic curves presented in Fig. 4A

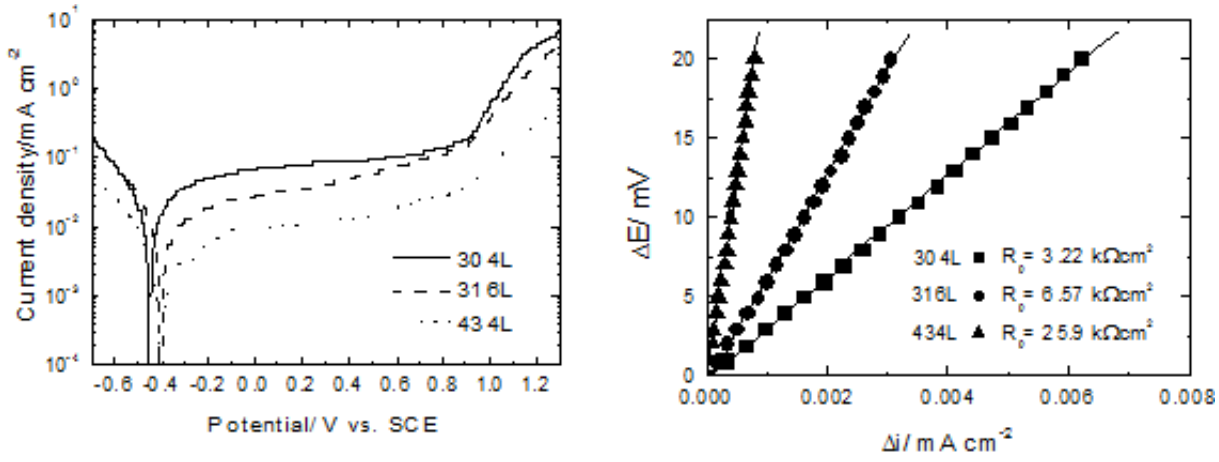

Fig. 5. A) Anodic polarization curves for sintered stainless steel obtained in 0.5 mol dm^{-3} Na_2SO_4, scan rate 1 mV s^{-1}, B) Change in the value of external current as a function of the applied voltage (within the range of E_{corr} + ΔE) for the analysed sinters on the basis of potentiokinetic curves presented in Fig. 5A

Corrosion resistance in sintered materials was also analysed in the solution of 0.5 mol dm^{-3} Na_2SO_4+ 0.5 mol dm^{-3} NaCl (Fig. 6A). Solution with pH = 4 containing 0.5 mol dm^{-3} of chloride ions limits precipitation of basic salts and inhibits, to a certain degree, active salt solubilisation. The values of the polarization resistance obtained for steel sinters indicate that the most resistant material is the sinter with ferritic structure, 434L (which is also characterized by the lowest porosity among the analysed sinters, see Fig. 8).

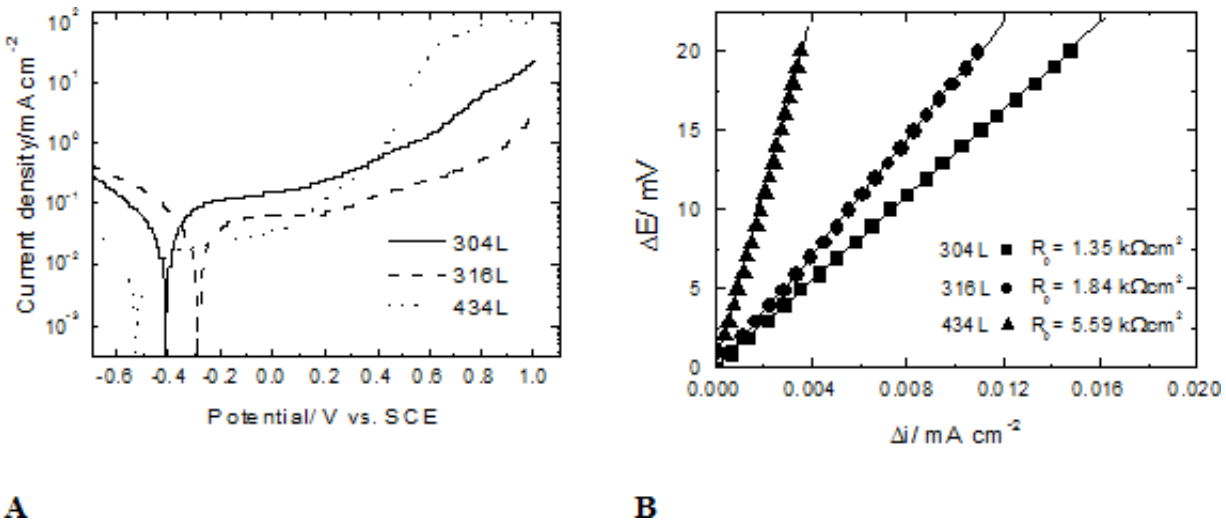

Fig. 6. A) Anodic polarization curves for sintered stainless steel obtained in 0.5 mol dm^{-3} Na_2SO_4+ 0.5 mol dm^{-3} NaCl , scan rate 1 mV s^{-1}, B) Change in the value of external current as a function of the applied voltage (within the range of $E_{corr} + \Delta E$) for the analysed sinters on the basis of potentiokinetic curves presented in Fig. 6A

TABLE 2

Results of electrochemical measurements in sintered materials

Sintered steel	Solution	E_{corr} [V]	i_{corr} [mA cm^{-2}]	R_p [Ω cm^2]
304L Austenitic structure	0.5 mol dm^{-3} H_2SO_4	-0.372	0.486	45.38
	0.5 mol dm^{-3} Na_2SO_4	-0.410	0.024	3.22· 10^3
	0. 5 mol dm^{-3} Na_2SO_4 + 0.5 mol dm^{-3} NaCl	-0.411	0.016	1.35· 10^3
316L Austenitic structure	0.5 mol dm^{-3} H_2SO_4	-0.311	0.195	88.41
	0.5 mol dm^{-3} Na_2SO_4	-0.279	0.028	6.57· 10^3
	0.5 mol dm^{-3} Na_2SO_4 + 0.5 mol dm^{-3} NaCl	-0.028	0.012	1.84· 10^3
434L Ferritic structure	0.5 mol dm^{-3} H_2SO_4	-0.510	0.846	16.28
	0.5 mol dm^{-3} Na_2SO_4	-0.524	0.007	25.9· 10^3
	0.5 mol dm^{-3} Na_2SO_4 + 0.5 mol dm^{-3} NaCl	-0.523	0.003	5.59· 10^3

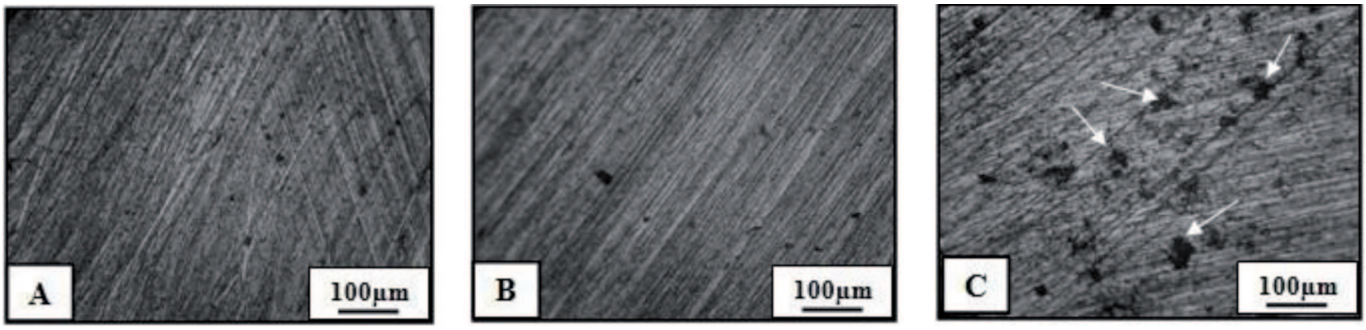

Fig. 7. Corrosive pits in microstructure of austenitic sintered steels A) 304L, B) 316L, and ferritic sintered steel C) 434L after exposition in corrosive solution of 0.5 mol dm^{-3} Na_2SO_4+ 0.5 mol dm^{-3} NaCl. Magnification 100x

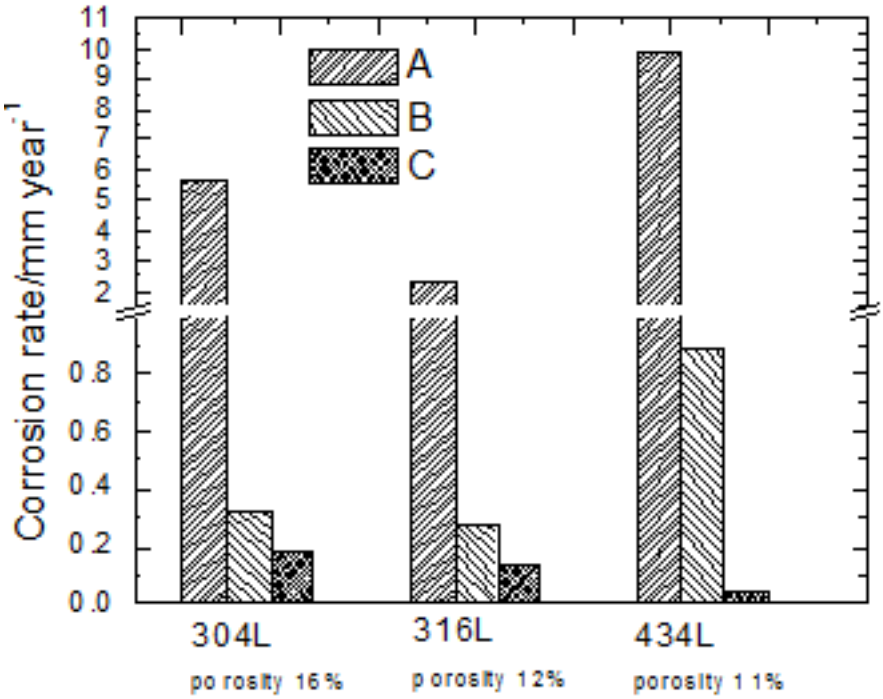

Fig. 8. Dependence of corrosion rate in the solutions of: A) 0.5 mol dm^{-3} H_2SO_4, B) 0.5 mol dm^{-3} Na_2SO_4, C) 0.5 mol dm^{-3} Na_2SO_4 + 0.5 mol dm^{-3} NaCl on material porosity

After an exposition of the sintered materials in the corrosive solution (0.5 mol dm^{-3} Na_2SO_4 + 0.5 mol dm^{-3} NaCl), the structural analysis of sinter surface was carried out (Fig. 7). The most distinct impact of chloride ions is observed for the 434L sinter with the ferritic structure (Fig. 7C). The corrosion pits observed in Fig. 7C are of irregular shape and are several times bigger as compared to the size of pits observed in the case of sinters with austenitic structure (304L and 316L).

Fundamental impact on corrosion properties of materials is from the porosity degree and their structure. Fig. 8 presents the effect of structural properties of the powders on the corrosion resistance in the sintered steels.

5. Summary

On the basis of the investigations, the following conclusions can be formulated:

– The powders used for preparation of the sinters were characterised by irregular dendritic structure of grain with comparable grain size (powders 304LHD and 316LHD). The 434LHC powder showed highest degree of particle surface development, 1.97.
– The results obtained on the basis of analysis of potentiokinetic curves and changes in the value of external current as a function of the applied voltage revealed that the corrosion resistance depends on the corrosive environment.
– The effect of chloride ions on sintered materials can be observed in the form of the number of corrosion pits and their shape after exposition of the material in corrosive solution.
– Considerable impact on corrosion resistance in the obtained sinters is from the material porosity and chemical composition.

Acknowledgements

Scientific work funded by the Ministry of Education and Science in the years 2008-2011 as a research project No. N N507 369235.

REFERENCES

[1] E. Antolini, Journal of Power Sources **170**, 1 (2007).
[2] V. Nebuchilor, J. Martin, H. Wang, J. Zhang, Journal of Power Sources **169**, 221 (2007).
[3] M. Chojak, M. Mascetti, R. Włodarczyk, R. Marassi, K. Karnicka, K. Miecznikowski, P.J. Kulesza, J. Solid State Electrochemistry **8**, 854 (2004).
[4] R. Włodarczyk, M. Chojak, K. Miecznikowski, A. Kolary, P.J. Kulesza, R. Marassi, Journal of Power Sources **159**, 802 (2006).

[5] P.J. Kulesza, B. Grzybowska, M.A. Malik, M. Chojak, K. Miecznikowski, Journal of Electroanalytical Chemistry **512**, 110 (2001).
[6] R. Włodarczyk, A. Kolary-Żurowska, R. Marassi, M. Chojak, P.J. Kulesza, Electrochimica Acta **52**, 3958 (2007).
[7] M. Chojak, A. Kolary-Żurowska, R. Włodarczyk, K. Miecznikowski, K. Karnicka, B. Pałys, R. Marassi, P.J. Kulesza, Electrochimica Acta **52**, 5574 (2007).
[8] Y.W. Rho, O.A. Velev, S. Srinivasan, Journal of Electrochemical Society **141**(8), 2084 (1994).
[9] Y.W. Rho, S. Srinivasan, Journal of Electrochemical Society **141**(8), 2089 (1994).
[10] C. Bernay, M. Marchand, M. Cassir, Journal of Power Sources **108**, 139 (2002).
[11] P. Kacejko, Generacja rozproszona w systemie elektroenergetycznym, Wydawnictwo Uczelniane PL, Lublin (2004).
[12] G. Demusiak, W. Warowny, Stacjonarne ogniwa paliwowe i ich zastosowanie w gospodarstwach domowych, Gaz, Woda i Technika Sanitarna **10**, 10 (2005).
[13] M. Guzenda, Niekonwencjonalne źródła energii, Ekologia, Energia Odnawialna, Ciepłownictwo w Polsce i na Świecie **5-6**, 77 (2004).
[14] J.R. Davis, ASM Handbook of stainless steel, Materials Park, OH: p. 238 ASM; 1994.

Received: 10 February 2011.